The Challenge of Surface Type Changes Over the Aral Sea for Satellite Remote Sensing of Precipitation

Quanhua Liu, Yong-Keun Lee, Christopher Grassotti, XingMing Liang, Stanley Q. Kidder, and Sheldon Kusselson

***Abstract*—Frequent false signals of precipitation in satellite passive microwave retrievals over the Aral Sea have been identified as being caused by an outdated surface database. The database includes the surface type, elevation, and the percentage of the primary surface type in each grid. It was also found that the grid resolution of 1/6 degree (∼18 km at the equator) of the outdated surface data was too coarse to process global precipitation measurement mission microwave imager data, which have a field of view resolution of 31.68 km^2 for channels at 89, 166.5, and 183.31 GHz). In this article, we generated a new surface database at a resolution of $0.05^\circ \times 0.05^\circ$ (∼5.6 km at the equator). Using the new surface data, the false precipitation problem above is addressed. At the same time, the retrieval accuracy for other parameters such as total precipitable water over the Aral sea is significantly improved as well. The resolution of the database is suitable for most microwave and infrared sounding measurements of atmospheric temperature and moisture profiles as well as precipitation. By comparing this new surface data against the outdated surface data, we also see the loss of permanent ice in Antarctica and a dramatic reduction of water surface over the Aral sea. Using a 40-year record of remote sensing data, we can observe the steady decrease in size of the Aral sea, as a result of regional water use policies and natural climate change.**

***Index Terms*—Aral sea, microwave integrated retrieval system (MiRS), surface type.**

I. Introduction

The Suomi National Polar-orbiting Partnership (SNPP) mission has delivered critical observations of the earth-atmosphere system since its launch on October 28, 2011 [1]. As a risk reduction mission, SNPP mission was the start of a new Earth observation system, the joint polar satellite system (JPSS). Subsequently, the first satellite, JPSS-1, now called NOAA-20, was successfully launched on November 18, 2017. JPSS [2] will provide continuity of critical global observations about climate change, air quality, natural disasters such as tornados, hurricanes, and wildfires through 2039 and beyond. Remote sensing data [3] play an important role in support of weather forecasting and the monitoring of environmental change. The National Oceanic and Atmospheric Administration (NOAA) Microwave Integrated Retrieval System (MiRS) generates daily 10 satellite products or environmental data records (EDRs) including precipitation rate from passive microwave measurements, such as the SNPP and NOAA-20 Advanced Technology Microwave Sounder (ATMS) instruments [4]. The ten EDRs greatly support the monitoring of severe weather and climate studies. However, environmental variations over time, such as water/land surface changes can challenge remote sensing data applications. We recently became aware (from a regular user of MiRS retrieval products) of a false precipitation signal in MiRS operational retrievals produced on August 17, 2021 over the Aral sea. The issue was carefully investigated and it was found that changes to water/land surface coverage was the root cause. We then checked the MiRS precipitation product back to 2020 and found the false signals of precipitation over Aral sea were quite frequent, occurring at least several times per month. MiRS uses a surface dataset, including 24 surface types, at 1/6° (∼18 km at the equator) resolution. Because the emissivity characteristics of land and water surfaces are so different in the millimeter and microwave spectral region, MiRS uses water/land information from the dataset to choose the appropriate a prior constraints and retrieval state vector basis functions. In particular, in the MiRS variational algorithm surface emissivity empirical orthogonal functions (EOFs) and the surface emissivity mean (a prior spectrum) as well as the error covariance matrix are dependent on the surface type. Because microwave emissivity of water is much lower than that over land, and has a different dependence on frequency, incorrect surface-type information can lead to improper prior constraints. This can pose problems for the retrieval because the inversion is an ill-posed problem (i.e., multiple possible solutions can correspond to the same set of measurements). The surface area of the Aral sea has been steadily shrinking since 1960 as the former Soviet Union converted large acreages of pastures into irrigated farmlands and diverting water that originally fed the Aral sea (https://www.britannica.com/place/Aral-Sea). In addition, changes to the regional climate have accelerated this trend. Precipitation over Aral sea decreased from 9.4 km^3 in 1960 to

Manuscript received 22 March 2022; revised 22 August 2022; accepted 30 September 2022. Date of publication 10 October 2022; date of current version 14 October 2022. This work was supported by NOAA Joint Polar Satellite System Program. *(Corresponding author: Quanhua Liu.)*

Quanhua Liu is with the NOAA Center for Satellite Applications and Research, National Environmental Satellite, Data, and Information Service, College Park, MD 20740 USA (e-mail: quanhua.liu@noaa.gov).

Yong-Keun Lee, Christopher Grassotti, and XingMing Liang are with the Cooperative Institute for Satellite and Earth System Studies, Earth System Science Interdisciplinary Center, University of Maryland, College Park, MD 20742 USA (e-mail: yong-keun.lee@noaa.gov; christopher.grassotti@noaa.gov; xingming.liang@noaa.gov).

Stanley Q. Kidder and Sheldon Kusselson are with the Cooperative Institute for Research in the Atmosphere, Colorado State University, Fort Collins, CO 80521 USA (e-mail: stanley.kidder@colostate.edu; sheldon.kusselson@colostate.edu).

Digital Object Identifier 10.1109/JSTARS.2022.3212647

3.2 km^3 in 2009 and to 2.1 km^3 in 2010 [5]. During a similar period, the water surface area decreased from 68 000 km^2 in 1960 to less than 10 000 km^2 in 2017 [6]. This significant change of water surface area poses challenges for the MiRS precipitation retrieval which currently uses static and historical land/water surface data. This article is organized as follows: We introduce the global surface type in Section II; Aral Sea's land and water surface change is described in Section III; Section IV discusses MiRS precipitation remote sensing; and Section VI leads to the summary and discussions.

II. Global Surface Type

Global surface-type classification and temporal changes to the surface classification provide critical information about climate change and human activities. In the 1990s, the International Geosphere–Biosphere Programme (IGBP) recommended IGBP surface-types using Advanced Very High-Resolution Radiometer (AVHRR) measurements [7]. The AVHRR red band at 0.615 $\mu\mathrm{m}$ and near infrared band at 0.912 $\mu\mathrm{m}$ [8] are good for calculating normalized difference vegetation index (NDVI) which strongly correlates with the greenness of surface vegetation. The NVDI [9] was defined as

$$\text{NVDI} = \frac{R_{\text{nir}} - R_{\text{red}}}{R_{\text{nir}} + R_{\text{red}}} \tag{1}$$

where R_{nir} and R_{red} are the reflectances or albedos of the AVHRR bands 2 and 1, respectively. Healthy vegetation (chlorophyll) reflects more near-infrared (NIR) and green light while it absorbs more red and blue light. Therefore, vegetation greenness is a measure of the healthiness of vegetation. NDVI has been used for many applications such as fraction of photosynthetically active radiation [10] and vegetation–climate interactions [11]. NDVI is the key parameter for determining global green vegetation fraction [12]. The NDVI is also an important parameter to the vegetation on land for IGBP surface-type classification [13], [14]. There are 17 IGBP surface types [15]. A total of 15 of 17 IGBP surface types depend on soil and vegetation.

In order to evaluate the existing surface-type datasets, we first received a dataset of 24 surface types in 1998 from National Polar-orbiting Operational Environmental Satellite System (NPOESS) Integrated program office. This dataset is called NPOESS surface data [16], however there appears to be no official documentation or publication which describes the origin of the NPOESS surface data. The dataset includes the surface elevation and the percentage of the primary surface type at a resolution of 1/6° ($\sim$18 km at the equator). A static surface reflectance database for the 24 surface types and wavelengths between 0.2 $\mu\mathrm{m}$ and 15 $\mu\mathrm{m}$ is also included with the surface-type data. The two datasets had been used to simulate the visible infrared imaging radiometer suite (VIIRS) radiances for the algorithm development and validation such as the sea surface temperature algorithm and the surface net heat flux algorithm. The databases are apparently useful and are still used by the NOAA MiRS [17] and the community radiative transfer model (CRTM) [18]. Further details about the MiRS algorithm are provided in Section IV.

The CRTM model, developed at the Joint Center for Satellite Data Assimilation, is an operational radiative transfer model in support of weather forecast and the generation of many EDRs. The CRTM model is widely used by numerical prediction centers, satellite retrieval products, and research and education communities. The CRTM embeds the surface reflectance for NPOESS 24 surface types. However, changes in surface type that may have occurred over at least the last 20 years are not included in the database, and the 1/6° resolution is inadequate for use with microwave imagery data such as GMI data. In this article, we use the latest NOAA surface-type data [19] derived from the VIIRS radiance data in 2020. There are 17 IGBP surface types [14]. The NOAA Environmental Modeling Center then added three tundra surface-types resulting in a total of 20 surface types. This dataset is called NOAA surface-type data. The NOAA surface-type dataset has a high spatial resolution of 1/120 degrees, which is needed for studying detailed surface types by using visible imagery observations. However, microwave sounding data have a coarse resolution. For example, the spatial resolution at nadir for the Advanced Microwave Sounding Unit-A (AMSU-A) is 48 km. The ATMS has a sample resolution of 16 km at nadir. Global precipitation measurement (GPM) microwave imager (GMI) high frequency channels have a high spatial resolution of 5.6 km for channel central frequencies higher than 89 GHz. In this article, we downscale the database surface type and elevation from 1/120° to 1/20° resolution. It should be pointed out that Aral Sea land/water masks in this 1/120 high resolution haven't been updated for many years. In this article, we directly derived the Aral sea land/water fraction from VIIRS radiance (see Section III) and included the land/water fraction in our surface-type data for MiRS retrieval system, which is called NOAA-MiRS surface-types hereafter.

III. Land & Water Change in Aral Sea

In this section, we focus on surface-type changes over the Aral sea. Aral sea was the fourth-largest freshwater lake in the world (https://en.wikipedia.org/wiki/Aral_Sea). In 1960, the water body had a surface area of 68 000 km^2 in 1960, larger than West Virginia of the United States. In this article, we used 40-year long (1981–2021) record of remote sensing data to estimate changes to the water surface area in the region. To do this we use red band reflectance and near-Infrared band reflectance from AVHRR, moderate resolution imaging spectroradiometer (MODIS), and VIIRS observations to compute the NDVI. The NDVI exploits the fact that over water, the red band reflectance is higher than near-infrared band reflectance, while the converse is true over land. The threshold NDVI value to distinguish land from water is a key parameter in the calculation of water surface area. The AVHRR does not have onboard calibrators for its red band and near-infrared band, and there are significant differences among the calibration of the various AVHRR instruments deployed on satellites [20]. However, rather than an absolute calibration, we only need to be able to identify the AVHRR NDVI features for each individual instrument. The AVHRR red band and near infrared band at a 4 km gridded data are used to calculate the NDVI. As shown in Fig. 1, the histogram of the weekly AVHRR

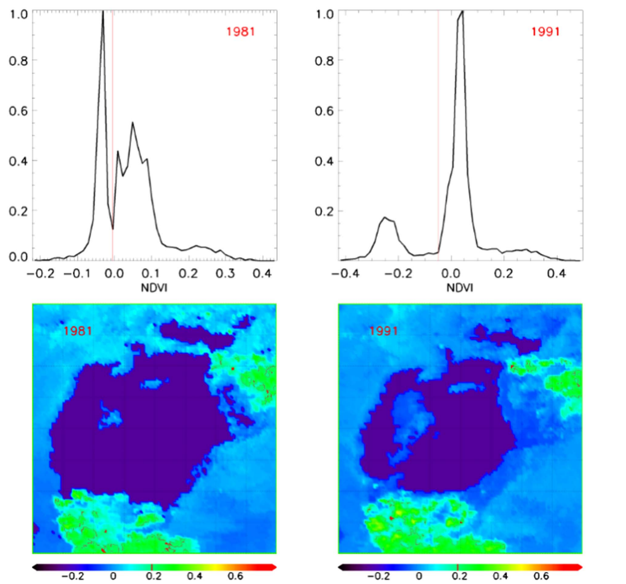

Fig. 1. Histogram of the AVHRR weekly normalized difference of vegetation index (NDVI) and the map of NDVI in the week 37 of 1981 (left) and in the week 35 of 1991 over Aral Sea for latitudes [43, 47] degrees and longitudes [58, 62] degrees. The dark blue color area on the maps are the pixels having NDVI less than the threshold (red line), which corresponds to water surface.

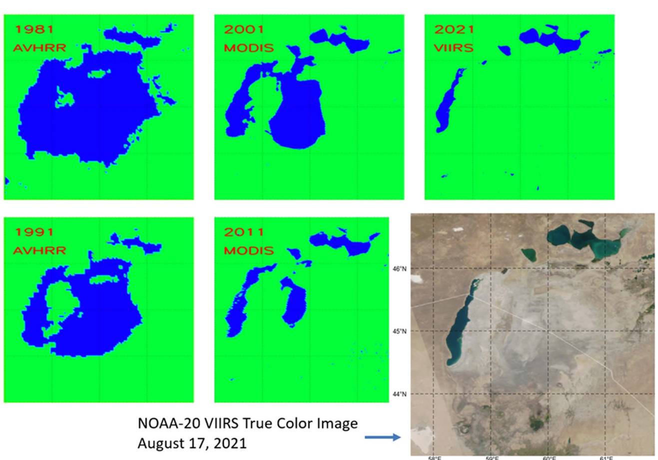

Fig. 2. Time series of Aral Sea surface type maps in the past 40 years. The NOAA-20 VIIRS true color image (bottom right) on August 17, 2021 is also included.

NDVI for NOAA-08 in the week 37 of 1981 (left image) and for NOAA-11 in the weekly 35 of 1991 (right image) shows distinguished surface features. The left and right sides of the red line are for water and land surface types, respectively.

MODIS imagery red band (channel at 645 nm) and near infrared band (channel 2 at 858 nm) have a spatial resolution of 250 meters at nadir. In comparison to the moderate spatial resolution bands, the imagery bands have better spatial resolution and its wide bandwidth are more suitable for studying vegetation and surface types. Using the NDVI histogram features for AVHRR and the threshold value of -0.05 for MODIS and VIIRS NDVI, we can calculate the water and land surface over the Aral Sea. In Fig. 2, we show the NDVI-derived surface classification, with water surface shown in blue and land surface in green.

TABLE I

Time Evolution of Aral Sea Water Surface Area Changes. AVHRR Weekly Data in 1981 (Week 37) and 1991 (Week 35) are Used. Daily MODIS Data on August 20, 2001, July 16, 2011 are Chosen. NOAA-20 VIIRS Data on August 17, 2021 is Used. Days Were Chosen Which Were Most Likely to Have Clear Skies

Year	Water Surface Area (km^2)	Percentage relative to 1960
1960	68,000	100%
1981	49,071 (AVHRR)	72.1%
1991	30961 (AVHRR)	45.5%
2001	21,913 (MODIS)	32.2%
2011	10,210 (MODIS)	15.0%
2021	4753 (VIIRS)	6.9%

One can observe from Fig. 2 that the water surface in the Aral Sea has decreased steadily and dramatically to a point where its size is a small fraction of its pre-1981 level. It has been shown in other studies that a minimum water surface area occurred in 2014 [21], [22], [23]. The size of water surface for 2021 in Fig. 2 is very similar to the minimum water surface area occurred in 2014. The 2021 derived surface type is also in very good agreement with the VIIRS true color image. Table I gives the water surface area in square kilometers and the water area percentage relative to the water surface area in 1960.

IV. Remotely Sensed Precipitation

MiRS has been run operationally at NOAA since 2007. MiRS has been generating m ultiple EDRs (i.e., satellite retrieval products) for NOAA satellites, European satellites Meteorological Operational Satellites Metop-B and Metop-C, GPM satellite and other satellites (https://www.star.nesdis.noaa.gov/mirs/highresolutionv.php). The satellite retrieval products include atmospheric profiles of temperature and water vapor, cloud liquid water, ice water content, rainfall rate, snow cover and snow water equivalent, snow fall rate, surface temperature and microwave emissivity, and sea ice concentration.

The retrieval is an ill-posed problem and the information content of the satellite observations is not sufficient to uniquely determine the solution for all atmospheric and surface parameters. Prior information such as the surface type greatly helps the retrieval system by imposing constraints on the solution including use of optimal EOF basis functions for surface emissivity and the emissivity error covariance matrix, since these constraints are surface-type dependent.

MiRS precipitation retrieval is based on the measured emission and scattering information from clouds. Rain drops are much larger than the particle size for non-precipitation clouds. The microwave scattering signatures increase as the cloud particle sizes increase. The surface type is also important in the retrieval process because it determines how the surface emissivity will be calculated and used in the radiative transfer model for simulating the brightness temperatures from state variables. The MiRS retrieval starts from nonprecipitation or an emission only mode. If no profile can be found to meet a convergence within

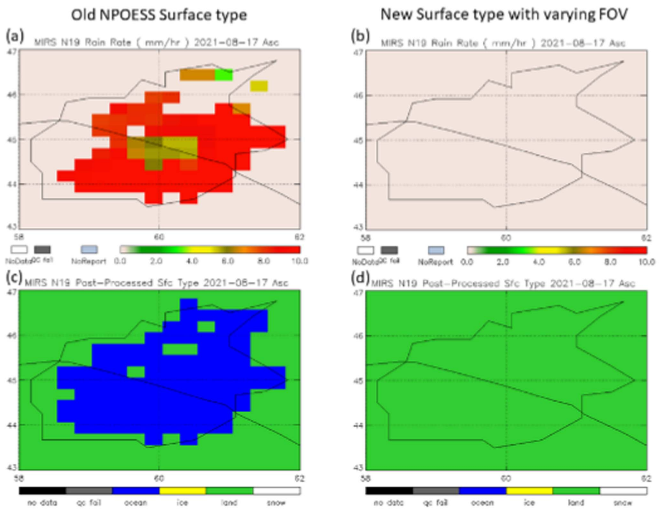

Fig. 3. MiRS retrieved surface rain rates and surface types over the Aral Sea area using NOAA-19 AMSU-A and MHS. Left panels show the result using the outdated surface type (NPOESS surface type) data in operations. (a) Rain rate in ascending orbits and (c) NPOESS surface type used in the MiRS retrieval procedure. Right panels show the result using new NOAA-MiRS surface types and also with a varying field of view size. (b) Rain rate in ascending orbits and (d) new surface type used the MiRS retrieval procedure. The results are valid on the date of August 17, 2021.

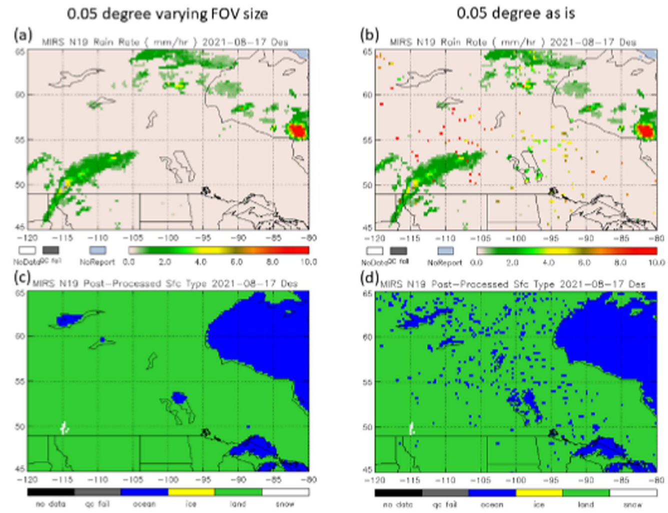

Fig. 4. Comparison of MiRS retrieved surface rain rates and surface types over Canada using NOAA-19 AMSU-A and MHS with the updated high resolution (0.05 degree) surface type database with (left columns) and without (right columns) consideration of field of view size. (a) and (b) Rain rates. (c) and (d) Surface types used in the MiRS retrieval procedure. The results are valid on the date of August 17, 2021. When field of view size is not considered a large amount of spurious precipitation is retrieved.

a defined number of iterations, the MiRS will start the second attempt with a small precipitation in a scattering mode. The convergence can be achieved when the difference between satellite measured and simulated brightness temperatures is smaller than a threshold that is typically comparable to the measurement uncertainty. Typical iteration number is 3 with an upper limit value of 7. The MiRS system works well. The global retrieval convergence level is about 95%.

The surface type is very important to MiRS because the surface emissivity between oceans and lands are very different. However, it is known that the surface type in the Aral Sea region has changed dramatically as the water body has shrunk in size (see Fig. 2). The Aral Sea land/water mask in the NPOESS surface data is very similar to land/water fraction for 1981 in Fig. 2. For determining surface type in the NOAA-MiRS dataset, the primary surface-type percentage is calculated from the VIIRS surface data within each 0.05° grid cell. Fig. 3 shows the MiRS derived surface type and MiRS retrieved surface precipitation over Aral Sea based on NOAA-19 AMSU-A and MHS data, corresponding to the use of two different surface databases are used: the original NPOESS surface data in Fig. 3(c), and the updated NOAA-MiRS dataset in Fig. 3(d). The surface types shown were used to determine a prior constraint in the retrieval as described above.

Most significantly, for the operational case of using the original NPOESS database, the MiRS precipitation in the upper-left map in Fig. 3 was confirmed as spurious based on surface observations and satellite true color images, which indicated mainly clear conditions. The false or spurious precipitation is directly related to the use of the outdated surface types. The outdated surface-type data shows a large portion of water surface in the center of the map. The new surface type does not show any water surface in the center region because the water coverage within the FOVs is less than 50% when the varying size of the AMSU-A FOVs is considered.

The second important factor is the footprint size of satellite measurements. The footprint size for most microwave sounders is larger than 15 km at nadir and increases with the zenith angles. The MiRS retrieval system only takes one surface type at the center point of each field of view. It is quite possible that the center point is water, for example a river or small lake, but the water area percentage is insignificant within the field of view. As one can see from the low right image in Fig. 4, there are many improper water surfaces to represent the satellite data footprints even we use the new surface with a high spatial resolution. Once we use the new surface-type data and consider the field of view size of satellite measurements, the improper water surfaces are removed (see lower left image in Fig. 4).

The false signals of the MiRS retrieved precipitation over Aral Sea were quite frequent. This article found that using the new surface-type data with a high spatial resolution, the false precipitations in the MiRS NOAA-19 products over Aral Sea on August 17, 2021 are removed. Both Global Precipitation Climatology Project (GPCP) daily precipitation analysis (https://www.ncei.noaa.gov/products/climate-data-records/precipitation-gpcp-daily) and the MiRS rain product by using the new surface-type data reported zero precipitation over Aral sea on August 17, 2021. The GPCP analysis is quite accuracy and can be used as a reference. However, the MiRS rain product by using the old surface-type data reported a mean rain rate of 7.83 and 6.61 millimeters for the same day for NOAA-19 ascending and descending orbits, respectively. The mean value is the averaged MiRS retrieved rain rate over a selected area

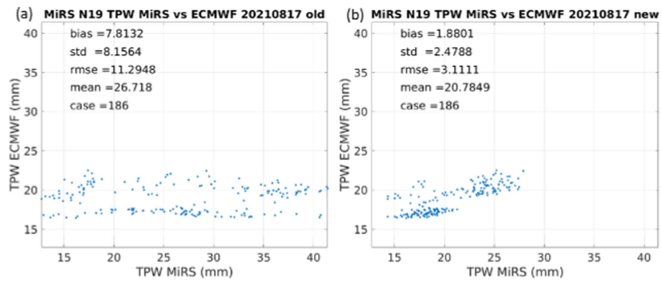

Fig. 5. Comparison of MiRS retrieved TPW against the ECMWF TPW analysis over the selected area over Aral Sea on August 17, 2021. Left panel is for the retrieval using the old surface type data. The right panel is for the retrieval using the new surface type data.

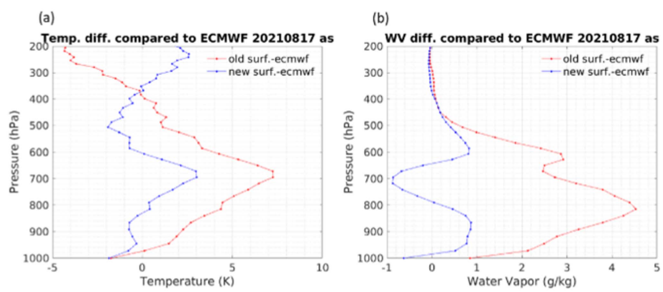

Fig. 6. Comparison of MiRS retrieved temperature (left) and water vapor (right) against the ECMWF analysis over the selected area over Aral sea on August 17, 2021. The red color curve is the comparison using the old surface type data. The blue color curve is the comparison using the new surface type data.

for the latitudes [44, 46] degrees north and longitudes [59, 61] degrees East.

Using the new surface-type data in the MiRS improved the retrieval accuracy for temperature and water vapor profiles as well as total precipitable water (TPW). Over the selected Aral Sea area above, the standard deviation error in MiRS retrieved TPW was reduced from 8.15 to 2.47 mm (see Fig. 5) by using the new surface-type data. The differences between European centre for medium-range weather forecasts (ECMWF) analysis and the MiRS retrieval for temperature and water vapor profiles are significantly reduced as well (see Fig. 6).

V. Discussion

The Aral sea was once the fourth-largest freshwater lake in the world. However, water use policies in the former Soviet Union in combination with regional climate changes resulted in reduced water inputs to the Aral SEA. Recent decreases in precipitation related to climate change has accelerated the reduction in size of the Aral sea. The surface-type change can also affect remote sensing applications in which surface type is an important source of a prior information. In this article, examination of a 40-year record of remote sensing data further confirms the significant reduction of Aral Sea water surface from 1981 to 2021. Our study found that this surface-type change related in part to climate change can impact remote sensing data applications. MiRS false precipitation retrievals over the Aral sea are an indirect consequence of climate change as the static ancillary surface database was not updated to account for local and temporal changes. To mitigate the risk, it is necessary to update prior static information frequently. We have generated surface data using 2020 VIIRS surface-type data and NOAA-20 VIIRS radiances over Aral sea. As shown in Fig. 2, for the Aral sea region, the NOAA-MiRS surface-type data have very good agreement with the VIIRS true color image. In addition, when implementing the higher spatial resolution database, it is critical that satellite FOV size is taken into account so that the database is sampled at the approximate spatial resolution of the satellite measurements.

Acknowledgment

The authors thank Dr. W. Guo very much for him to provide AVHRR weekly NDVI data and Dr. X. Zhan, Dr. Y. Yu, and Dr. W. Zhang for their valuable comments and suggestions. We also thank J. Forsythe for highlighting the precipitation retrieval anomalies over the Aral Sea. This article was supported by Joint Polar Satellite System Program. The manuscript contents are solely the opinions of the authors and do not constitute a statement of policy, decision, or position on behalf of NOAA or the U.S. government.

References

[1] X. Xiong and J. Butler, "MODIS and VIIRS calibration history and future outlook," *Remote Sens.*, vol. 12, 2000, Art. no. 2523. [Online]. Available: https://doi.org/10.3390/rs12162523

[2] L. Zhou, M. Divakarla, X. Liu, A. Layns, and M. D. Goldberg, "An overview of the science performances and calibration/validation of joint polar satellite system operational products," *Remote Sens.*, vol. 11, 2019, Art. no. 698. [Online]. Available: https://doi.org/10.3390/rs11060698

[3] W. Yang, "A review of remote sensing data formats for earth system observations," in *Earth Science Satellite Remote Sensing*, J. J. Qu, W. Gao, M. Kafatos, R. E. Murphy, and V. V. Salomonson, Eds. Berlin, Germany: Springer, 2006. [Online]. Available: https://doi.org/10.1007/978-3-540-37294-3_7

[4] C. Grassotti et al., "Precipitation estimation from the microwave integrated retrieval system (MiRS)," in *Satellite Precipitation Measurement. Advances in Global Change Research*. vol. 67, V. Levizzani, C. Kidd, D. Kirschbaum, C. Kummerow, K. Nakamura, and F. Turk, Eds. Cham, Switzerland: Springer, 2006. [Online]. Available: https://doi.org/10.1007/978-3-030-24568-9_9

[5] B. Gaybullaev, S. C. Chen, and D. Gaybullaev, "Changes in water volume of the Aral Sea after 1960," *Appl. Water Sci.*, vol. 2, pp. 285–291, 2012. [Online]. Available: https://doi.org/10.1007/s13201-012-0048-z

[6] X. W. Yang, N. L. Wang, A. A. Chen, J. He, T. Hua, and Y. F. Qie, "Changes in area and water volume of the Aral sea in the arid central Asia over the period of 1960–2018 and their causes," *Catena*, vol. 191, 2020, Art. no. 104566.

[7] T. R. Loveland, B. C. Reed, J. F. Brown, D. O. Ohlen, Z. Zhu, and L. Yang, "Development of a global land cover characteristics database and IGBP discover from 1 km AVHRR data," *Int. J. Remote Sens.*, vol. 21, pp. 1303–1330, 2000.

[8] C. Li et al., "Post calibration of channels 1 and 2 of long-term AVHRR data record based on SeaWiFS data and pseudo-invariant targets," *Remote Sens. Environ.*, vol. 150, pp. 104–119, 2014.

[9] H. E. Beck, T. R. McVicar, A. I. van Dijk, J. Schellekens, R. A. de Jeu, and L. A. Bruijnzeel, "Global evaluation of four AVHRR-NDVI data sets: Intercomparison and assessment against landsat imagery," *Remote Sens. Environ.*, vol. 115, pp. 2547–2563, 2011.

[10] K. P. Gallo, C. S. T. Daughtry, and M. E. Bauer, "Spectral estimation of absorbed photosynthetically active radiation in corn canopies," *Remote Sens. Environ.*, vol. 17, pp. 221–232, 1985.

[11] R. J. Donohue, T. R. McVicar, and M. L. Roderick, "Climate-related trends in Australian vegetation cover as inferred from satellite observations, 1981–2006," *Glob. Change Biol.*, vol. 15, pp. 1025–1039, 2009.

[12] L. Jiang et al., "Real-time weekly global green vegetation fraction derived from advanced very high resolution radiometer-based NOAA operational global vegetation index (GVI) system," *J. Geophys. Res.*, vol. 115, 2010, Art. no. D11114.

[13] D. L. Sun and M. Kafatos, "Note on the NDVI-LST relationship and the use of temperature-related drought indices over North America," *Geophys. Res. Lett.*, vol. 34, 2007, Art. no. L24406.

[14] S. Guha and H. Govil, "Land surface temperature and normalized difference vegetation index relationship: A seasonal study on a tropical city," *SN Appl. Sci.*, vol. 2, 2020, Art. no. 1661.

[15] C. Q. Huang, R. Zhang, X. Zhan, and I. Csiszar, "Derivation of global surface type products from VIIRS," in *Proc. IEEE Int. Geosci. Remote Sens. Symp.*, 2019, pp. 5992–5995.

[16] X. Zhuge, X. Zou, and Y. Wang, "A comparison between three surface type data sets adopted by the community radiative transfer model," *Remote Sens. Lett.*, vol. 8, pp. 801–810, 2017.

[17] S.-A. Boukabara et al., "A physical approach for a simultaneous retrieval of sounding surface, hydrometeor, and cryospheric parameters from SNPP/ATMS," *J. Geophys. Res. Atmos.*, vol. 118, pp. 12,600–12,619, 2013.

[18] Q. Liu and S.-A. Boukabara, "Community radiation transfer model (CRTM) applications in supporting the suomi national polar-orbiting partnership (SNPP) mission validation and verification," *Remote Sen. Environ.*, vol. 140, pp. 744–754, 2014. [Online]. Available: https://doi.org/10.1016/j.rse.2013.10.011

[19] R. Zhang, C. Huang, X. Zhan, Q. Dai, and K. Song, "Development and validation of the global surface type data product from S-NPP VIIRS," *Remote Sens. Lett.*, vol. 7, pp. 51–60, 2016.

[20] C. R. N. Rao and J. Chen, "Inter-satellite calibration linkages for the visible and near-infared channels of the advanced very high resolution radiometer on the NOAA-7, -9, and -11 spacecraft," *Int. J. Remote Sens.*, vol. 16, no. 11, pp. 1931–1942, 1995.

[21] J. F. Pekel, A. Cottam, N. Gorelick, and A. S. Belward, "High-resolution mapping of global surface water and its long-term changes," *Nature*, vol. 540, pp. 418–422, 2016. [Online]. Available: https://doi.org/10.1038/nature20584

[22] W. Shi and M. Wang, "Decadal changes of water properties in the Aral Sea observed by MODIS-Aqua," *J. Geophys. Res. Oceans*, vol. 120, pp. 4687–4708, 2015.

[23] P. Micklin, "The Aral Sea disaster," *Annu. Rev. Earth Planet. Sci.*, vol. 35, pp. 47–72, 2007.

Quanhua Liu received the B.S. degree from the Nanjing University of Information Science and Technology (former Nanjing Institute of Meteorology), Nanjing, China, in 1982, the Master's degree in physics from the Chinese Academy of Science, Beijing, China, in 1984, and the Ph.D. degree in meteorology and remote sensing from the University of Kiel, Kiel, Germany, in 1992.

He was a Senior Research Scientist with the University of Maryland (College Park, MD), working as the co-Chair of the Community Radiative Transfer Model, USA. He is a Physical Scientist with the NOAA/NESDIS Center for Satellite Applications and Research. He is leading NOAA ATMS sensor data record calibration and NOAA Microwave Integrated Retrieval System that retrieves 10 environmental data records. His research interests include radiative transfer models, satellite products, and sensor calibration and climate studies.

Yong-Keun Lee received the B.S. and M.S. degrees in atmospheric science from Seoul National University, Seoul, South Korea, and the Ph.D. degree in atmospheric science from Texas A&M University, College Station, TX, USA.

From 2006 to 2018, he was with the Space Science and Engineering Center, University of Wisconsin. Since 2018, he has been with the Earth System Science Interdisciplinary Center, University of Maryland, College Park, MD, USA, and the National Oceanic and Atmospheric Administration, NOAA Center for Satellite Application and Research, National Environmental Satellites, Data, and Information Service, College Park, MD, USA.

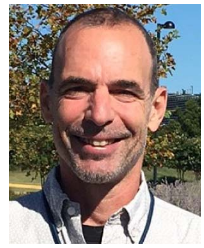

Christopher Grassotti received the B.S. degree in earth and space science from the State University of New York, Stony Brook, NY, USA, the M.S. degree in meteorology from the University of Wisconsin-Madison, Madison, WI, USA, and the M.S. degree in viticulture and enology from AgroMontpellier, Montpellier, France.

From 1986 to 1991 and again from 1993 to 2005, he was a Research Associate and Senior Research Associate with Atmospheric and Environmental Research, Inc. From 1991 to 1993, he was with the Atmospheric Environmental Service, Environment Canada in Dorval, QC, Canada. Since 2008, he has been with the National Oceanic and Atmospheric Administration, NOAA Center for Satellite Application and Research, National Environmental Satellite, Data, and Information Service, College Park, MD, USA.

XingMing Liang received the B.S. degree in construction machinery from Jilin University, Changchun, China, in 1992, and the Ph.D. degree in remote sensing and atmospheric sciences from Saga University, Saga, Japan, in 2005.

He was a Research Scientist with the Cooperative Institute for Research in the Atmosphere, Colorado State University, Fort Collins, CO, USA, from 2007 to 2016. He was a Senior Scientist with Earth Resources Technology, Inc., and Global Science and Technology Inc., from 2016 to 2019. He is currently an Assistant Research Scientist with the Cooperative Institute for Satellite Earth System Studies, University of Maryland, College Park, MD, USA, and works at the Center for Satellite Applications and Research of NOAA/NESDIS on developing Artificial intelligence applications in remote sensing and supporting the development of the Microwave Integrated Retrieval System and the community radiative transfer model.

Stanley Q. Kidder received the B.S. degree in physics from Harvey Mudd College in 1971 and the M.S. and Ph.D. degrees in atmospheric science from Colorado State University, Fort Collins, CO, USA, in 1976 and 1979, respectively.

He was with the University of Illinois and the University of Alabama in Huntsville as well as with Colorado State University and COMET. He was a Senior Research Scientist with the Cooperative Institute for Research in the Atmosphere, Colorado State, since 1996. He is the author (with Dr. T. H. Vonder Haar) of the book Satellite Meteorology: An Introduction, (Academic Press, 1995). His research interests include the application of satellite data to meteorological problems.

Sheldon Kusselson received the B.S. degree in meteorology from Pennsylvania State University, University Park, PA, USA, in 1975.

He had the unique experience during his 36 years working in NOAA/NESDIS to both support forecasters with expert satellite analysis and applications, especially for heavy precipitation and flood hazard mitigation and at the same time collaborate with government and university researchers to develop and improve satellite products that forecasters can use to improve the timeliness and accuracy of heavy precipitation forecasts. This is a true Research to Operations and Operations to Research environment that has paid huge benefits to the forecasters across the country who are responsible everyday in carrying out NOAA's mission of protecting lives and property. In retirement, he works part time for the Cooperative Institute for Research in the Atmosphere (CIRA)/Colorado State University providing his expertise in satellite moisture applications and analysis for the development of new and improving existing satellite moisture products.